J. Fluid Mech. (1969), *vol.* 37, *part* 1, *pp.* 51–80
Printed in Great Britain

Turbulent buoyant convection from a source in a confined region

By W. D. BAINES† AND J. S. TURNER
Department of Applied Mathematics and Theoretical Physics,
University of Cambridge

(Received 11 July 1968)

This paper considers the effect of continuous convection from small sources of buoyancy on the properties of the environment when the region of interest is bounded. The main assumptions are that the entrainment into the turbulent buoyant region is at a rate proportional to the local mean upward velocity, and that the buoyant elements spread out at the top of the region and become part of the non-turbulent environment at that level. Asymptotic solutions, valid at large times, are obtained for the cases of plumes from point and line sources and also periodically released thermals. These all have the properties that the environment is stably stratified, with the density profile fixed in shape, changing at a uniform rate in time at all levels, and everywhere descending (with ascending buoyant elements).

The analysis is carried out in detail for the point source in an environment of constant cross-section. Laboratory experiments have been conducted for this case, and these verify the major predictions of the theory. It is then shown how the method can be extended to include more realistic starting conditions for the convection, and a general shape of bounded environment. Finally, the model is applied quantitatively to a variety of problems in engineering, the atmosphere and the ocean, and the limitations on its use are discussed.

1. Introduction

Most work in the field of free convection has been developed from two rather different concepts of the motion produced by buoyancy forces. First, there are the studies of convection between parallel plates heated below and cooled above which have extended the work of Bénard on cellular convection to conditions of higher heat flux and turbulent flow. In these, the emphasis has largely been on the mean motions and the statistical properties for the case of steady mean temperature, that is, heat flux constant with height. Until very recently little attention has been paid to the details of the processes through which these are achieved. On the other hand there are the theories and experiments which examine the properties of individual convection elements such as buoyant plumes. These phenomena have been studied for a variety of environmental

† While on leave from the Department of Mechanical Engineering, University of Toronto.

conditions but usually with the assumption, stated or implied, that the density distribution in the environment can be specified in advance, and that it is unchanged during the period of interest, i.e. that the environment is effectively infinite compared to the scale of the plumes rising through it.

In the present paper we shall discuss a simple model of the convective process which has something in common with both the above: namely, convection from sources placed in a finite closed region. This model can take into account several features which are arbitrarily and often unreasonably neglected in the earlier work. For example, although the atmosphere very near the ground can be treated as if the heat flux were nearly steady and constant with height, this assumption is poor when the whole surface layer (up to cloud-base) is considered. This layer is heated up by a few degrees during a morning of strong convection, and most of this heating is due to the solar heating at the ground which means that the heat flux is certainly not constant with height. It becomes obvious, too, when experimenting with plumes in the laboratory that experimental tanks (and even the atmosphere) are far from infinite. Fluid which has been in the plume soon spreads out and modifies the environment, and can in turn alter the subsequent behaviour of the plume. A time-dependent solution which takes into account the interaction between the buoyant elements and the environment is clearly required.

Another feature of convection in confined regions difficult to understand using the conventional models is that the environment away from boundaries is often slightly stable in the mean. This has been observed in the atmosphere by Warner & Telford (1967), and seems to be generally true in the so-called 'upper mixed layer' of the ocean even under conditions when convective overturning would be expected. Another oceanographic example is the pool of hot salty water at the bottom of the Red Sea (to which a more detailed reference will be made in § 5.3); this seems to be heating from below, but at the same time maintaining a slightly stable density gradient (Pugh 1969).

In the laboratory a reversal of the temperature gradient across the central region in horizontal parallel plate convection experiments has been observed, in agreement with the results of numerical calculations (for example, see Herring 1964). A particularly clear demonstration of this phenomenon has been given recently by Gille (1967) using an optical method. Also of interest here are the experiments of Schwind & Vliet (1964) who studied the motions and the stratification produced in closed tanks by the heating of the vertical side walls. Their results, and the explanation they gave of them, have much in common with those to be described here, though they did not produce a detailed theory.

In all of these cases a stable environment is associated with the transfer of heat (or buoyancy) against the mean gradient. This is inexplicable if one thinks entirely in terms of the mean distributions and a steady state, but it emerges as a natural consequence of this time and space dependent model which accounts explicitly for the buoyant elements.

2. A physical description of the model

Before the detailed theory is presented, it will be helpful to give a qualitative description of the model, based on the laboratory experiments used later to make the quantitative tests of the theory. In this way we can introduce the basic idea and demonstrate its plausibility in a practical case, and at the same time discuss the simplifying assumptions used in the analysis.

2.1 *The laboratory experiment*

The experiment consists simply of supplying concentrated salt solution at a steady rate to a small nozzle projecting just below the surface of an aquarium tank of fresh water, and allowing the resulting turbulent plume to run for a very long time. The volume of added salt is negligible compared to the total volume of the tank, and the source velocity is small, so the source approximates to one of buoyancy alone. At various stages neutrally buoyant dye is added to mark a patch of fluid which had been in the plume at a particular time. The first heavy fluid to reach the bottom spreads out and produces a layer with a discontinuity or front above it, marked by dye in figure 1 (*a*), plate 1. The turbulence in this layer quickly dies out, and as far as the continuing plume is concerned, it acts as part of the non-turbulent environment. Because the layer is heavier than the original fresh water, the plume which entrains it arrives at the bottom of the tank even heavier, and slides underneath. The first front is pushed upwards, and if more dye is injected this too will spread out in a layer and be lifted in its turn. Figure 1 (*b*), plate 1, shows a later stage of the same experiment, during the fifth injection of dye. All the previously marked layers are clearly visible.

It is not at all obvious that the tank should begin to fill with heavy fluid in this way. One can ask why a large scale vertical circulation is not set up instead, which mixes the salt solution from top to bottom. This question will be pursued later; it is sufficient to say now that a general overturning can occur if the inertia of the plume as it reaches the bottom is large compared with the buoyancy forces. This form of motion is favoured by regions which are deep compared to their width (or to the typical spacing of plumes) and is more likely to happen in the two-dimensional case.

Returning now to the experiment, several important properties of our model can be deduced from the pictures shown in figure 1. The environmental density distribution built up in this way is certainly stable. After a long time the whole of the environment consists of fluid which has at some time been in the dyed plume. This is being entrained again into the plume producing a general lifting† of the environment. Because of the stable density distribution this lifting produces a continuous increase in density at any level. The dye sheets in figure 1 (*b*), which were injected at equal time intervals, are much closer together near the

† It should be noted, in order to avoid confusion later, that the theory will be presented and detailed comparison with experiments made assuming the direction of motion in the plumes is *upwards*. This is a more familiar convention and more useful for the major application to the atmosphere, but it nevertheless seems desirable to describe the experiments here as they were actually carried out.

top of the tank, but are moving more and more slowly. It will be shown later that they mark approximately equally spaced density surfaces, so this observation means that the density gradient is sharpened as the source is approached, due to the continuous removal of fluid between any two levels by entrainment into the plume.

Considering the conservation of mass and buoyancy one deduces that the pattern outlined in figure 2 must have developed. Below the first front the density and salinity (or temperature) are constant at the initial value and at this front there must be a step change. At all other places in the environment the density variation is smooth and continuous.

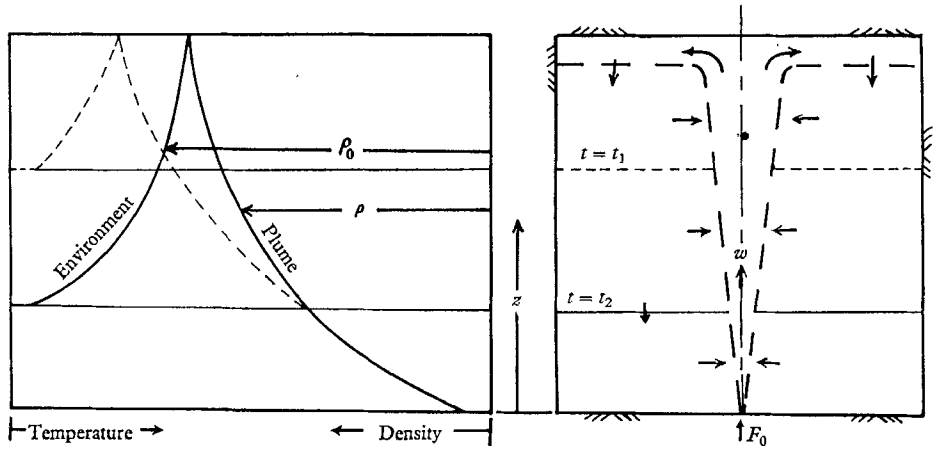

FIGURE 2. Sketch of development of stratified environment due to a heat source, showing the motions in the plume and environment, and the corresponding temperature profiles at two times. The horizontal lines indicate the positions of the first front.

This experiment gives some support to the basic assumption on which the present work is based: that the whole of the properties of the environment, as well as the plumes themselves, should be calculable once the geometry and the strengths of buoyancy sources are known. In order to make progress theoretically, we have had to make more restrictive assumptions which are discussed below.

2.2. *The idealized model*

Point or line sources of buoyancy will be assumed here for mathematical convenience, though the same methods can be applied equally well to finite sources. The main development of the ideas will be carried out for the steady axisymmetric plume, the case which is most easily tested in the laboratory, but results will also be given more briefly for a line plume and suddenly released axisymmetric 'thermals'. First of all we will treat a rectangular region, or more accurately one in which the cross-sectional area does not change with height, but later we will show how the method can easily be generalized to include other shapes of basin. It will be assumed that when the plume fluid reaches the top or (bottom) of the box, it spreads out instantaneously into a thin horizontal layer; the actual process of sideways flow will be ignored. The stable stratification will suppress any

turbulence and mixing in the environment, and it will also be assumed strong enough for the fluid entrained into the plume at any level to come entirely from the environment at that level, i.e. 'draw down' effects will be ignored.

The most important physical assumption is that the inflow into the plume is proportional to the local mean velocity in the plume. This has been used to solve other problems of convection in stratified fluids, and it has been discussed in detail elsewhere (Morton, Taylor & Turner 1956). Finally, we shall restrict the discussion to two special features of the motion and not attempt the general time dependent problem. The motion of the first front can be solved exactly since it depends only on the properties of the plume in the uniform environment ahead of the front. The behaviour in the rest of the region will be calculated only for the asymptotic state achieved after a long time when the whole of the fluid in the environment has been affected by passing through the plume. In this state it emerges that the density gradient has a distribution with height which remains fixed in time, while the density at all levels is increasing linearly with time through the mechanism of vertical motion in the stable environment. The plume properties in this state are also constant in time.

3. The circular plume

3.1. *The basic equations*

In addition to the use of a point source of buoyancy alone, and the entrainment assumption relating the velocity of inflow to the mean velocity in the plume, we shall also require the usual assumptions that the density differences are everywhere small except in the buoyancy terms, and that the profiles of mean vertical velocity and of mean buoyancy are similar at all heights. It will be assumed that the profiles are of Gaussian form and of equal width

$$\left.\begin{aligned} \bar{w}(z,r) &= w(z)\exp(-r^2/b^2) \\ \text{and} \qquad g(\rho_0-\rho(z,r))/\rho_1 &= \Delta(z)\exp(-r^2/b^2), \end{aligned}\right\} \tag{1}$$

where the z-axis is positive upwards, r is a radial co-ordinate, ρ and ρ_0 are the densities inside and outside the plume and ρ_1 is some standard reference density for the system, which by assumption can never be very different from ρ_0 anywhere. Thus w, the mean velocity on the axis, and b, the radius at which this has fallen to $1/e$ of its central value, are used as the velocity and length scales for the plume. The whole treatment can equally well be carried out using scales defined by the integrals of volume and momentum fluxes across the plume, which is equivalent to the use of 'top hot' profiles, and allowance can be made too for unequal spread of velocity and buoyancy (Morton 1959). Nothing is fundamentally changed by the choice made here, since the form of the equations stays the same and only numerical constants will be different. The whole analysis will be carried out for incompressible fluids, but as usual it can be applied to the compressible atmosphere by replacing density by potential density.

The equations of conservation of volume, momentum and density deficiency in the plume integrated over the section for the Gaussian profiles, reduce to the

following set derived by Morton *et al.* (1956), if it is assumed that the velocities in the plume are much larger than those in the environment, an approximation which will be justified below.

$$\left.\begin{aligned} \frac{d}{dz}(b^2w) &= 2\alpha bw, \\ \frac{d}{dz}\left(\frac{b^2w^2}{2}\right) &= b^2\Delta, \\ \frac{d}{dz}\left(\frac{b^2w\Delta}{2}\right) &= b^2w\frac{\partial\Delta_0}{\partial z}. \end{aligned}\right\} \tag{2}$$

Here α is the entrainment constant, chosen to make the rate of entrainment of volume at any height equal to $2\pi b\alpha w$. The density gradient in the environment is taken into account in the last term, which is defined by

$$\partial\Delta_0/\partial z = (g/\rho_1)(\partial\rho_0/\partial z), \quad \Delta_0 = g(\rho_0-\rho_1)/\rho_1.$$

In a closed region of depth H and cross-sectional area πR^2 (see figure 2) two other relations will be satisfied. The downward volume flux in the environment at any level must equal the upward flux in the plume, which gives

$$-\pi R^2U = \pi b^2w, \tag{3}$$

if it is assumed that $R^2 \gg b^2$, i.e. the area containing plumes is a small fraction of the total area at any level. The same assumption also ensures that the vertical velocity U in the environment can be neglected in the momentum equations for the plume. Secondly, we have

$$\partial\Delta_0/\partial t = -U(\partial\Delta_0/\partial z), \tag{4}$$

expressing the fact that density changes in the environment at any level occur only because of the vertical motion, not because of any mixing or diffusion.

3.2. *The first front*

When one is interested in the rate of advance of the front of buoyant fluid which first reaches the upper boundary and begins to descend, it is necessary to use only the equations for a uniform fluid. For it is clear from figure 2 that all the fluid added to the region above the front must have come originally by the entrainment into the plume in the uniform region below; recirculation of buoyant fluid will have no effect on the front. The properties of the plume below the front can be expressed in the usual way in terms of powers of z and the (constant) buoyancy flux

$$F_0 = \tfrac{1}{2}\pi b^2w\Delta|_{z=0},$$

$$b = \tfrac{6}{5}\alpha z, \quad w = \frac{5}{6\alpha}\left(\frac{18}{5\pi}\alpha F_0\right)^{\frac{1}{3}}z^{-\frac{1}{3}}, \quad \Delta = \frac{5}{3\pi}\left(\frac{5\pi}{18}\right)^{\frac{1}{3}}\alpha^{-\frac{4}{3}}F_0^{\frac{2}{3}}z^{-\frac{5}{3}}. \tag{5}$$

The density step at the front at all times is just that in the plume when it reaches the top, i.e. it is obtained by putting $z = H$ in the above expression for Δ;

$$\Delta_H = \frac{5}{3\pi}(\tfrac{5}{18}\pi)^{\frac{1}{3}}\alpha^{-\frac{4}{3}}F_0^{\frac{2}{3}}H^{-\frac{5}{3}}.$$

The velocity of the front $dz_0/dt = U$ is obtained when (3) and (5) are applied at this level.

Integration gives the relation between the position z_0 of the front and the time t in which this is attained (measuring from the time the plume first reached the top)

$$t = \frac{5}{4\alpha}\left(\frac{5\pi}{18\alpha}\right)^{\frac{1}{3}} R^2 H^{-\frac{2}{3}} F_0^{-\frac{1}{3}}\left[\left(\frac{H}{z_0}\right)^{\frac{2}{3}} - 1\right]. \tag{6}$$

This will be written in a non-dimensional form (consistent with the notation to be used later)

$$\tau = 5(\tfrac{5}{18})^{\frac{1}{3}}[\zeta_0^{-\frac{2}{3}} - 1], \tag{6a}$$

in which

$$\zeta = \frac{z}{H} \quad \text{and} \quad \tau = \frac{4}{\pi^{\frac{1}{3}}}\alpha^{\frac{4}{3}}\left(\frac{H}{R}\right)^2 \frac{F_0^{\frac{1}{3}}}{H^{\frac{4}{3}}} t. \tag{7}$$

It is now possible to discuss approximately the conditions under which our model is relevant, or when a general overturning could take place instead of the filling process pictured here. We must relax the assumption of infinitely fast spreading of the fluid at the top of the box and consider a mixed layer with thickness about b in which a density difference Δ builds up during the time the plume fluid moves to the side walls of the tank. The stabilizing buoyancy force per unit mass on this layer is $B = \pi R^2 b \Delta_H$. The inertial force due to the arrival of plume fluid at the upper boundary is $I = \frac{1}{2}\pi w^2 b^2$. If one supposes that this momentum flux could be deflected downwards a measure of the tendency towards overturning is the ratio I/B which is given by (5) as

$$\frac{I}{B} = \frac{9}{10}\alpha\left(\frac{H}{R}\right)^2. \tag{8}$$

Large values of this ratio imply instability and although this calculation is too crude for the constants to be significant, the main result is probably valid; overturning is not to be expected except in relatively tall regions.

Some simple experiments in which the ratio H/R was varied showed that the form of the instability is present but not so simple as envisioned in the analysis. As the ratio was steadily increased the well-mixed layer near $\zeta = 1$ increased in thickness and a pattern of overturning developed. This was observed as a flow from the outer part of the well-mixed bottom layer toward the plume with a definite upward component. For $H/R = 1$ this was not discernable but for $H/R = 1{\cdot}5$ could be seen clearly. The zone from $\zeta = 0{\cdot}5$ to $\zeta = 1{\cdot}0$ was filled with a non-uniform ring vortex motion and the zone to $\zeta = 0$ was a stratified quasi-static region as described in § 2. For $H/R = 2{\cdot}0$ the motion in the overturning layer was noticably stronger and the quasi-static region extended only to $\zeta = 0{\cdot}3$. It was further reduced to $\zeta = 0{\cdot}2$ for $H/R = 2{\cdot}5$. From these observations it is concluded that $H/R = 1$ is the largest value for which this analysis is fully valid and that the limiting value of the parameter in (8) is about 0·1.

3.3. *Theory for the asymptotic state*

We will now consider the solution of the full set of equations (2), (3) and (4). A similarity solution can be found in which only Δ_0, the environmental density,

depends on time while b, w, U and Δ are functions of ζ but not of time. This solution is approached asymptotically after an infinite time, but requires only small modification for practical situations. On a plot similar to figure 2 the density profiles would remain a constant shape but advance to the right at a uniform rate.

Time can be eliminated from (4) if Δ_0 is assumed to be linear in t. This is also a reasonable assumption physically, since the result of steady heating for a long time should be a uniform increase in temperature through the whole of the environment. The physical variables can be expressed as non-dimensional functions of τ and ζ defined in (7) by scaling with the given physical parameters of the problem, F_0 and H. The following transformations have been chosen to bring the equations to their simplest non-dimensional form:

$$\left.\begin{aligned} \Delta_0 &= (4\pi)^{-\frac{2}{3}} F_0^{\frac{2}{3}} \alpha^{-\frac{4}{3}} H^{-\frac{5}{3}} [f_0(\zeta) - \tau], \\ \Delta &= (2\pi)^{-\frac{2}{3}} F_0^{\frac{2}{3}} \alpha^{-\frac{4}{3}} H^{-\frac{5}{3}} f(\zeta), \\ w &= (2\pi)^{-\frac{1}{3}} F_0^{\frac{1}{3}} \alpha^{-\frac{2}{3}} H^{-\frac{1}{3}} g(\zeta), \\ b &= 2\alpha H h(\zeta), \\ U &= 4\pi^{-\frac{1}{3}} F_0^{\frac{1}{3}} \alpha^{\frac{4}{3}} H^{-\frac{1}{3}} (H/R)^2 j(\zeta). \end{aligned}\right\} \tag{9}$$

Substitution into (3) shows that $j = -gh^2$. If we define $k = gh$, then the four differential equations (2) and (4) take the non-dimensional form

$$dj/d\zeta = -k, \tag{10a}$$

$$dk^2/d\zeta = h^2 f, \tag{10b}$$

$$d(fj)/d\zeta = j\,df_0/d\zeta, \tag{10c}$$

$$j(df_0/d\zeta) = 1. \tag{10d}$$

These last two equations can be combined to give a single equation for the non-dimensional buoyancy flux fj in the plume, whose integral

$$fj = -(1-\zeta) \tag{11}$$

satisfies the proper boundary conditions at $\zeta = 0$ and $\zeta = 1$. The flux falls linearly from its value at the source to zero at $z = H$, as it must if the environment is heating up uniformly. Using (11) with (10b) gives a pair of equations to be solved together for j and k:

$$\left.\begin{aligned} dj/d\zeta &= -k, \\ k^2(dk^2/d\zeta) &= -j(1-\zeta). \end{aligned}\right\} \tag{12}$$

When j is obtained (10d) can then be integrated to give f_0 as a separate step.

The two remaining boundary conditions to be imposed on (12) are that $j = 0$ and $k = 0$ at $\zeta = 0$. These imply that the solutions near the origin are of the same form as for a point source in uniform surroundings. Series solutions can be obtained which quickly converge over the whole range of integration $0 \leqslant \zeta \leqslant 1$. The first three terms of the solution for j and k are:

$$\left.\begin{aligned} -j = gh^2 &= 0{\cdot}459\zeta^{\frac{5}{3}} - 0{\cdot}0588\zeta^{\frac{8}{3}} - 0{\cdot}0100\zeta^{\frac{11}{3}}, \\ k = gh &= 0{\cdot}765\zeta^{\frac{2}{3}} - 0{\cdot}157\zeta^{\frac{5}{3}} - 0{\cdot}0366\zeta^{\frac{8}{3}}. \end{aligned}\right\} \tag{13}$$

The coefficients of the leading terms of these series are just those needed to make the chosen forms (9) compatible with the solutions (5) in uniform surroundings. All functions except f_0 can be calculated algebraically from (11) and (13), and integration of (10d) gives

$$f_0 = \zeta^{-\frac{2}{3}}(3{\cdot}27 - 0{\cdot}837\zeta - 0{\cdot}062\zeta^2) - 2{\cdot}37. \tag{14}$$

The constant of integration has been determined by arbitrarily setting $f_0 = 0$ at $\zeta = 1$. A constant might be determined by considering the establishment of this state, and another would result from the definition of ρ_1, but these have been ignored.

These solutions are shown in figure 3. Note that the sign of j is reversed for convenience of plotting. The infinity in f_0 at $\zeta = 0$ is the consequence of $U \to 0$ as $\zeta \to 0$, i.e. fluid particles never reach the lower surface where the source is located; it is not present when more realistic boundary conditions are imposed, as will be shown later.

An additional result which is most convenient for comparison with the experimental results is the time taken for a marked layer of fluid to travel from the boundary where the plume spreads out ($\zeta = 1$) to a general level ζ, the whole motion taking place after the asymptotic state has been achieved. In dimensional form this is $t = \int_H^z dz/U$ and so the relation in the non-dimensional functions is

$$\tau = \int_1^\zeta \frac{d\zeta}{j} = f_0\Big|_1^\zeta = f_0(\zeta), \tag{15}$$

choosing the constant to make $\tau = 0$ at $\zeta = 1$ to this order of approximation. Thus the time history of a fluid layer in the environment gives a second measure of the asymptotic density distribution.

3.4. *Labaratory experiments with axisymmetric plumes*

The laboratory equipment used was so simple that little description is needed additional to that given in § 2. The transparent tank used was rectangular, 57·7 cm × 42·7 cm cross-section and 45 cm deep. Experiments were carried out with nozzles placed at 20 cm, 30 cm and 40 cm above the bottom of the tank, with the initial level of fresh water about 0·5 cm above this. After analysis of some exploratory runs, for which a nozzle of about 1 mm diameter was used, showed that (6) could not be satisfied, it was concluded that the momentum of the plume was too large. For all of the data shown herein a nozzle of 5 mm diameter was used. This was as large as could be used giving uniform and steady flow but it is not certain that momentum effects are completely absent. To determine this a more extensive study would be required in which the Froude number of the finite source varied systematically. The salt solution used was 13–16 % heavier than fresh water. A constant head tank and flowmeters were used to control and measure the rate of addition of salt water, and hence the buoyancy flux F_0.

As the experiment was started 1 ml of fluorescent dye was added to the plume. This remained (as shown in figure 1) in a distinct layer which marked the first front of fluid affected by the plume. It was observed by lighting through a slit

across the top of the tank, and its position was recorded as a function of time by measuring against two vertical scales, one right in the centre of the tank underneath the illuminated slit, and the other behind to minimize parallex errors. The origin of time $t = 0$ was arbitrarily taken as the instant the marked fluid reached the side of the tank. In the early stages it was difficult to measure heights

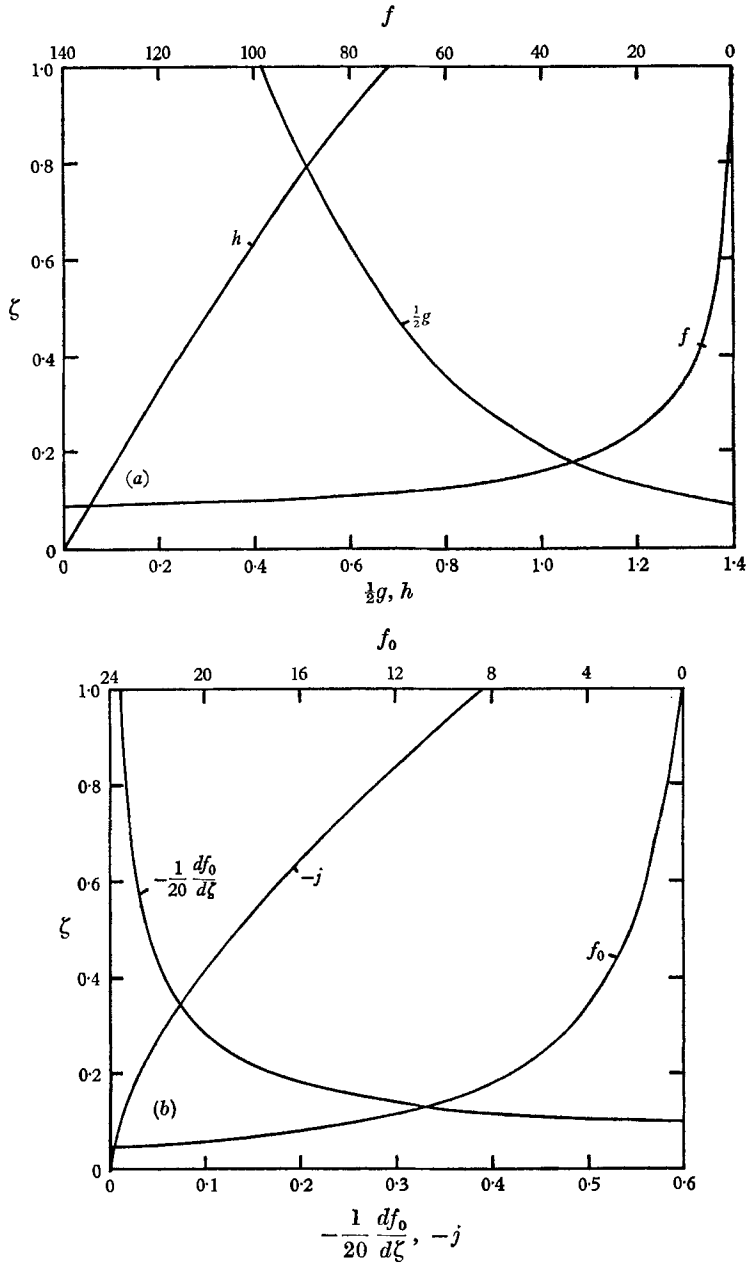

FIGURE 3. Asymptotic solutions for circular plume. (*a*) Plume velocity g, radius h, and density defect f defined by (9). (*b*) Environment velocity j, density gradient $df_0/d\zeta$ and density defect f_0 defined by (9).

more accurately than to $\pm 0{\cdot}5$ cm, because of waves on the interface, but as the interface rose, its position could be defined to $\pm 0{\cdot}1$ cm. At later times, when the first front approached the source, the interface became so sharp that optical distortion made an accurate determination more difficult.

When the first front had risen so close to the source that it appeared reasonable to assume that the asymptotic state had been reached in most of the environment, a second patch of dye was added, and followed as before. After this, too, had risen through most of the depth of the tank, the supply of salt was turned off.

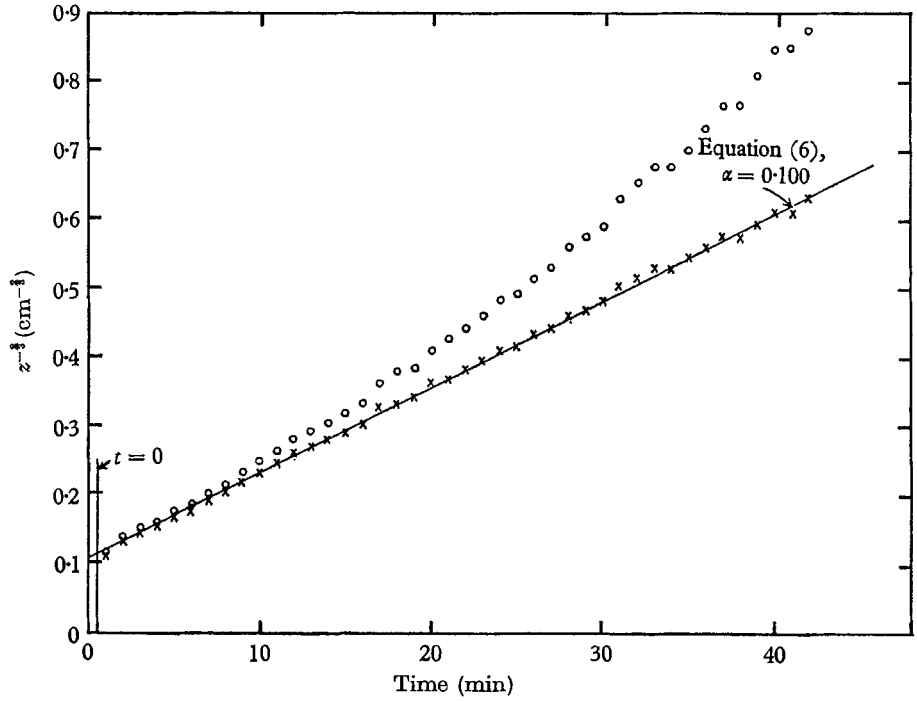

FIGURE 4. Measured progress of first front. Method used to establish virtual origin is demonstrated. ○, $z = 0$ at end of nozzle; ×, virtual source 0·8 cm behind nozzle.

Small samples of fluid were withdrawn from six to eight levels in the tank, and weighed to determine the density distribution. The two time sequences and the density distribution, for experiments carried out with two flow-rates and three depths, constitute the raw data which we wish now to compare with the theoretical predictions.

The first front data have been plotted in a form suggested by (6), $z_0^{-\frac{2}{3}}$ against t. If the distance from the real nozzle is used it does not, in general, produce a straight line; but the addition of a constant length does make it possible to obtain an accurately linear plot, as shown in figure 4. This then is a sensitive method for finding the position of the virtual source; and the intercept and slope of this line also allow one to make estimates of two other parameters which enter into the theory. The 'effective depth' of the box H is more plausibly defined as z for $t = 0$ rather than by using the actual depth, because of the finite thickness of the

layer which spreads out along the boundary. The value of α which emerges from the measurements on all the 'first fronts' is $\alpha = 0{\cdot}10$ (appropriate for Gaussian profiles). This is even larger than the value of 0·093 suggested by the small scale experiments of Morton *et al.* (1956) in stratified surroundings, which is itself larger than the value of 0·083 obtained from profile measurements by Rouse, Yih & Humphreys (1952) in air. In principle the accurate measurement of the first front behaviour gives a sensitive *direct* method of determining α (which has yet to be done for axisymmetric plumes), and this would be well worth doing on a larger scale for its own sake.

For the present purposes the value of $\alpha = 0{\cdot}10$ found experimentally will be used throughout the data reduction. All the first front results are plotted non-dimensionally in figure 5, with ζ_0 against the functional form suggested by (7), but without the numerical constant (which includes α). This constant is taken into account only in the placement of the line, which is the theoretical prediction (6). The symbols on figure 5 denote particular values of flux and depth of tank. These are listed in table 1.

Symbols used on figures 5–7	Depth (cm)	H (cm)	F_0 (cm^4/sec^5)	τ_1	τ_2
▽	20	17·5	66	62·4	124·8
△	20	19	117	51·8	103·6
◑	30	27·5	141	58·4	131·3
◐	30	27·5	77	56·4	142·4
⊡	40	32·5	128	74·8	153·5
◇	40	36	81·3	57·7	133·5
◈	40	36	81·3	—	433

TABLE 1. Summary of experimental conditions

Plotting the results for the motion of the second layer of dye in the same dimensionless form gives the agreement with (6a) as shown in figure 6. The time of marking this layer after the start of the experiment is listed as τ_1 on table 1. The values of α and H determined from the first front have been used but the origin of time defined when $z = H$. This has forced these points and those on figure 5 to be coincident for small t but the procedure was necessary, since the direct determination of when the coloured fluid reached the edge of the tank could not be done accurately because of the disturbances due to internal waves and turbulence.

It is evident that the plots on figures 5 and 6 are quite similar and it is found that the time for given ζ on figure 6 is very nearly 1·11 that on figure 5. That is, the first front travels about 11 % faster than the ones marked at large times. This small difference in velocity explains in part why the asymptotic state is reached so quickly; as soon as the first front has passed, the density gradient at any level is very close to that in the asymptotic state.

Finally, the directly measured density distributions in the environment, scaled according to (9), have been plotted together in figure 7 where they are

compared with the theoretical prediction (14). The point corresponding to the density on the boundary $\zeta = 1$ has been kept fixed, but otherwise there is no arbitrariness in either the curve for the theory or the experimental points. The time τ_2 in table 1 is the time the distribution was measured after the start of the experiment. The results are close to the theoretical curve for the shallower depths but not for the deepest case. No observations during the experiment would

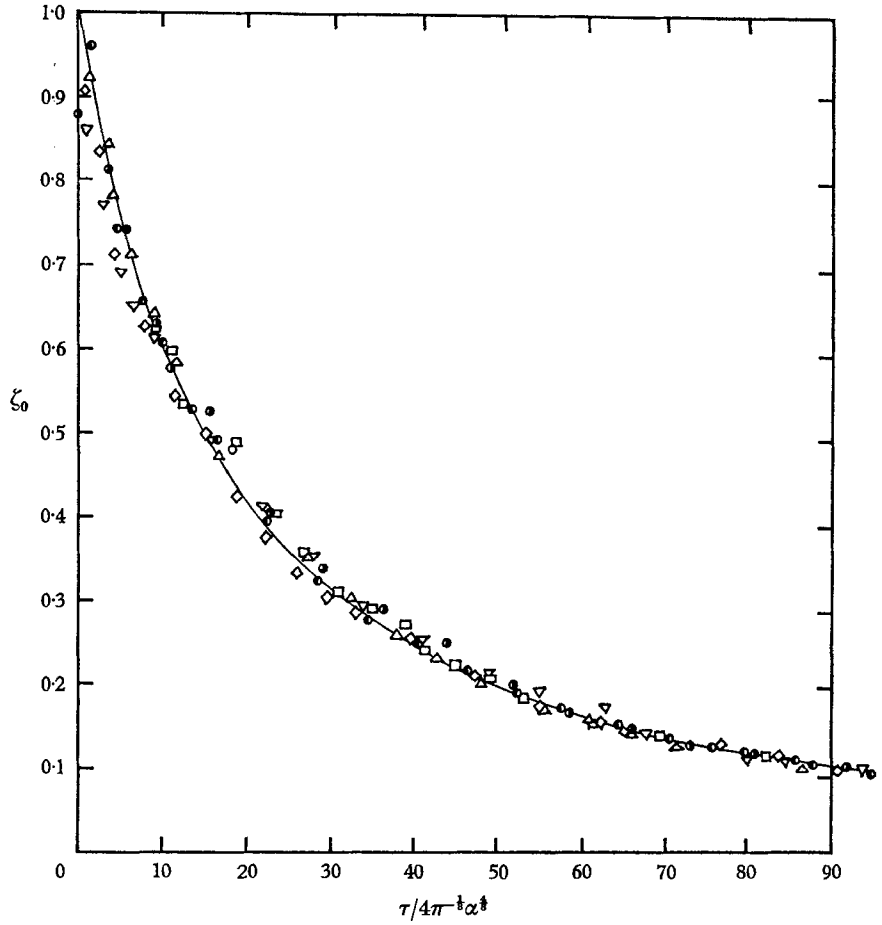

FIGURE 5. Dimensionless position of first front. Points are identified in table 1, line is (6*a*) with $\alpha = 0{\cdot}100$.

suggest the reason for this deviation. It is in the direction to be expected if the duration were too short, but another run was made for a time four times as great and as can be noted on figure 7 the results were virtually identical. Perhaps the deviation is due to mixing by turbulence in the layer spreading along the bottom of the tank which was probably relatively large, this case being closest to the instability limit.

4. Other types of sources

Buoyancy sources of other geometries are as easy to treat theoretically. Results for two of them will be briefly derived here. An extensive experimental verification of these results has not been attempted though a preliminary test of one case will be reported.

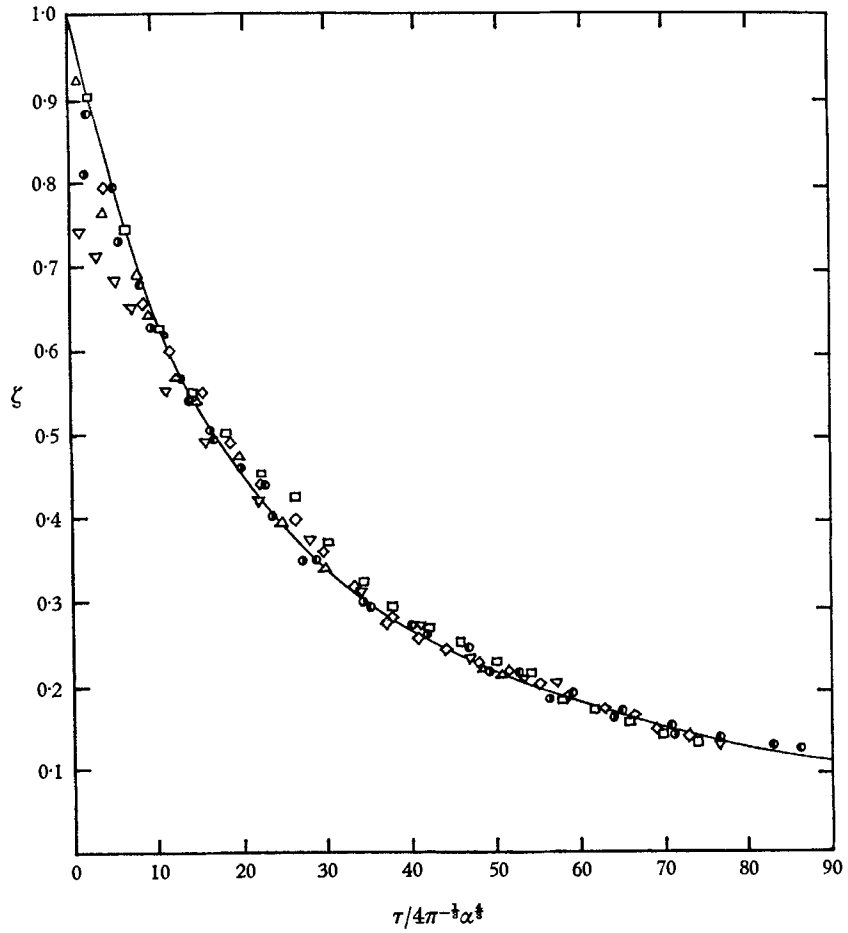

FIGURE 6. Dimensionless position of subsequent front. Line is (15) with $\alpha = 0{\cdot}100$.

4.1. *The line plume*

Gaussian profiles have again been adopted and similar assumptions made; the only change is that the plume and environment behaviour must depend now on the buoyancy flux $F_0 = \sqrt{(\pi/2)}\, bw\Delta|_{z\to 0}$ per unit length as well as the depth H and width $2R$ of the two-dimensional box. We shall proceed straight to the non-dimensional equations to which the three plume equations and the two de-

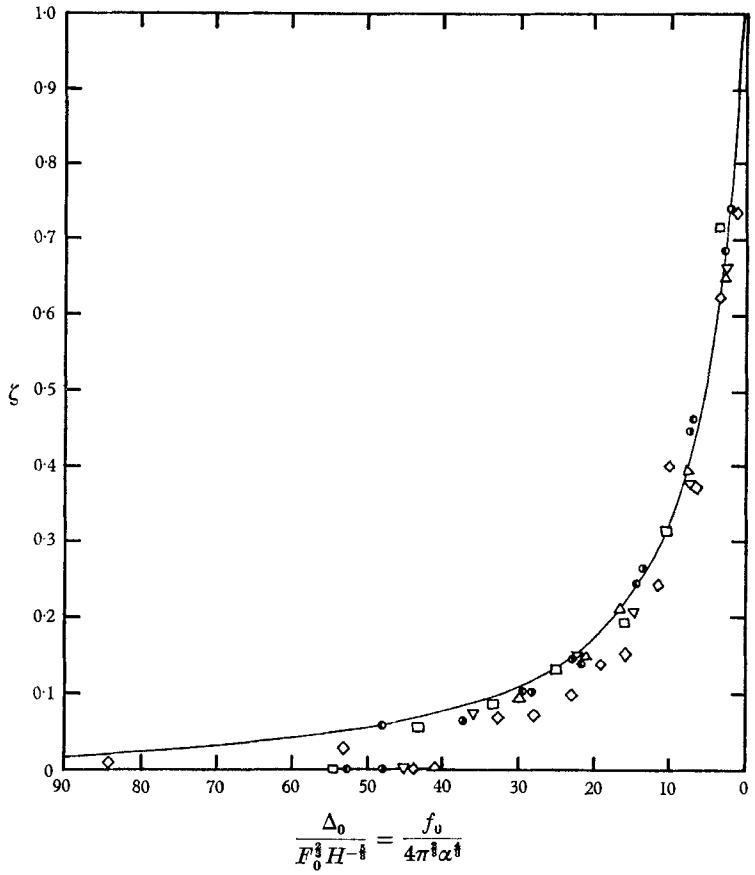

FIGURE 7. Dimensionless density defect distribution compared to theory, (14) with $\alpha = 0{\cdot}100$.

scribing the environment reduce if one defines the non-dimensional functions of $\zeta = z/H$ by:

$$\left.\begin{aligned} \Delta_0 &= 2^{-\frac{1}{3}}F_0^{\frac{2}{3}}\alpha^{-\frac{2}{3}}H^{-1}[f_0(\zeta)-\tau], \\ \Delta &= 2^{\frac{1}{6}}F_0^{\frac{2}{3}}\alpha^{-\frac{2}{3}}H^{-1}f(\zeta), \\ w &= 2^{\frac{1}{3}}F_0^{\frac{1}{3}}\alpha^{-\frac{1}{3}}g(\zeta), \\ b &= \pi^{-\frac{1}{2}}\alpha H h(\zeta), \\ U &= 2^{-\frac{2}{3}}F_0^{\frac{1}{3}}\alpha^{\frac{2}{3}}(H/R)j(\zeta), \\ t &= 2^{\frac{2}{3}}F_0^{-\frac{1}{3}}\alpha^{-\frac{2}{3}}R\tau. \end{aligned}\right\} \tag{16}$$

The dimensionless differential equations are:

$$dj/d\zeta = -g, \tag{17a}$$

$$d(gj)/d\zeta = -fh, \tag{17b}$$

$$d(fj)/d\zeta = j(df_0/d\zeta), \tag{17c}$$

$$j(df_0/d\zeta) = 1 \tag{17d}$$

with the subsidiary algebraic relation $j = -gh$ (which follows from the equation of continuity in the environment). As before, (17*c*) and (17*d*) combine to give

$$fj = -(1-\zeta), \tag{18}$$

satisfying the boundary conditions on f at the top and bottom. Substituting in (17*b*) leads to a pair of equations in j and $jg = -g^2h = x$, say

$$\left.\begin{aligned} j(dj/d\zeta) &= -x, \\ x(dx/d\zeta) &= -j(1-\zeta). \end{aligned}\right\} \tag{19}$$

Series solutions which satisfy the boundary conditions and from which all the properties of interest can be obtained, are

$$\left.\begin{aligned} j &= -\zeta + \tfrac{1}{8}\zeta^2 + \tfrac{3}{160}\zeta^3 + \ldots, \\ x = jg &= -\zeta + \tfrac{3}{8}\zeta^2 + \tfrac{7}{160}\zeta^3 + \ldots, \\ f_0 &= 0{\cdot}1422 - \log\zeta - \tfrac{1}{8}\zeta - \tfrac{11}{640}\zeta^2 \ldots. \end{aligned}\right\} \tag{20}$$

The last relation was obtained by a further integration, the constant being evaluated by setting $\Delta_0 = 0$ at $z = H$. The non-dimensional solutions are plotted in figure 8. Near the source, these again approach the conditions in uniform surroundings. The time taken for a layer of marked fluid to move from the top $\zeta = 1$ to the level ζ is readily shown to be the same as (15).

$$\tau = f_0(\zeta)$$

by combining (17*d*) with the definition $j = d\zeta/d\tau$. The descent of the first front can again be discussed entirely in terms of the motion of the plume in the uniform environment ahead of the front. The calculation is simpler here, since the two-dimensional plume has a constant velocity; the non-dimensional result is

$$\tau = \ln \zeta_0^{-1}. \tag{21}$$

In this case too it is useful to consider the stability of the flow, or when a general overturning is to be expected. The buoyancy force per unit mass and width on a layer which spreads out with depth b is $B = 2Rb\Delta$, and the inertial force is $I = \sqrt{(\pi/2)}\, w^2 b$; arguing as before the ratio

$$I/B = 0{\cdot}5H/R \tag{22}$$

should give a measure of the tendency to overturn. The constant is uncertain, but (22) suggests that the critical condition now depends purely on the geometry of the region, not on the flux or other properties (or even on α). An attempt was made to confirm this relationship in a rectangular box 60 cm wide and 20 cm deep which had a 2·5 cm wide electrically heated line source in the centre of the base. The box was filled with air and the flow pattern observed for various heights. With the ratio of the depth to the half-width set at two, one single rotating cell was observed which filled the box. For the ratio of 1·3 there were two cells giving a pattern symmetrical about the centre line. The vorticity in the environment was evident and the largest velocities were seen down the walls and along the

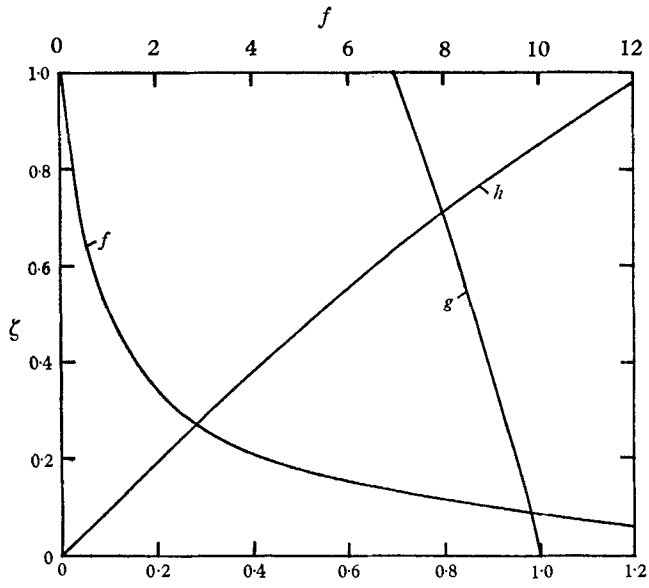

(*a*)

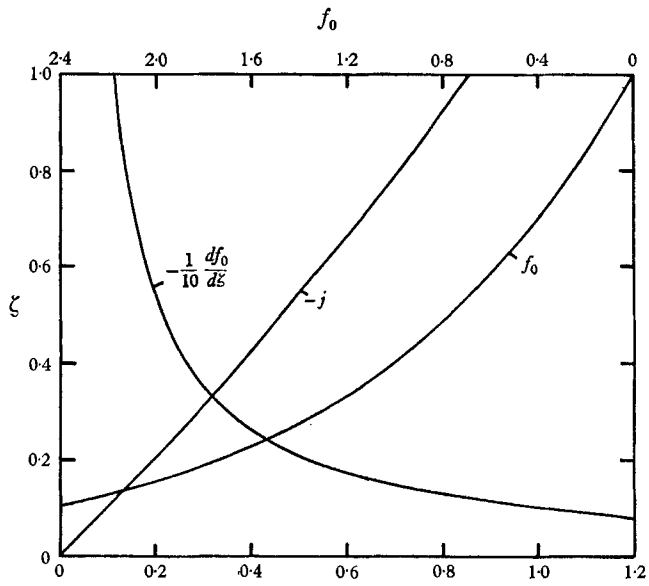

(*b*)

FIGURE 8. Asymptotic solutions for line plume in container of constant cross section. (*a*) Plume variables defined by (16). (*b*) Environment variables defined by (16).

floor. When the ratio was reduced to one or less this vorticity could not be noted and the environment appeared to have the motion assumed in this analysis. Thus it is concluded that critical value of H/R is about one. The exact value could not be determined from these experiments since the location of neither the virtual source nor the virtual top of the box could be readily determined. The critical value of the parameter in (22) is therefore about 0·5.

4.2. *The suddenly released point source or 'thermal'*

If buoyancy is released in the form of a succession of identical thermals (assumed here for convenience to be spherical), each having buoyancy $F_0 = 4\pi b^3\Delta/3|_{z\to 0}$, the analysis is especially simple. In this case it can be shown using the entrainment assumption and the continuity equation (Morton *et al.* 1956) that $b = \alpha z = \alpha H\zeta$ whatever the conditions of stratification, where α is an entrainment constant relating the inflow velocity to the mean upward velocity. With the assumption of a spherical region of buoyant fluid (which can be modified if necessary) and similarity of profiles of velocity and buoyancy at all heights, Turner (1963) has shown that the equations of momentum and continuity of density deficiency can be written in the form:

$$\frac{d}{dt}(b^3w) = \tfrac{2}{3}b^3\Delta, \quad \frac{d}{dt}(b^3\Delta) = b^3w\frac{d\Delta_0}{dz}, \tag{23}$$

in which w and Δ specify the mean values in the spherical region.

In the environment, which is again of depth H and cross-sectional area πR^2, the equation of conservation of Δ_0 is exactly the same as for the plumes, (4), but with the descent velocity U taken as a short term time average. That is, the thermals are released at a rate of n per unit time and the environment conditions are averaged over the time interval $1/n$. Thus the other environment equation which expresses the equality of volume flux for the upward and downward motions is

$$n\tfrac{4}{3}\pi b^3 = -\pi R^2 U,$$

which gives the environment velocity U directly:

$$U = -\tfrac{4}{3}n\alpha^3(H^3/R^2)\,\zeta^3. \tag{24}$$

After combining with (4) and the averaged rate of increase of buoyancy

$$\partial\Delta_0/\partial t = -nF_0/\pi R^2 H, \tag{25}$$

(24) defines the environment buoyancy gradient

$$\frac{\partial\Delta_0}{\partial z} = -\frac{3}{4\pi}\frac{F_0}{H^4\alpha^3}\frac{1}{\zeta^3}. \tag{26}$$

This can be integrated directly giving

$$\Delta_0 = \frac{3}{8\pi^3}\frac{F_0}{H^3}(\zeta^{-2} - 1 - \tau), \tag{27}$$

where $\tau = (3t/8\alpha^3 n)\,(R/H)^2$ is the dimensionless time variable. Inserting these

expressions into the second of (23) produces an equation which is directly integrated to give

$$\Delta = \frac{3}{4\pi}\frac{F_0}{H^3\alpha^3}\frac{1-\zeta}{\zeta^3}, \tag{28}$$

where the boundary condition $\Delta = 0, z = H$ has been used. The first of (23) can in turn be integrated directly for the thermal velocity

$$w = \sqrt{\left(\frac{F_0}{2\pi\alpha^3}\right)}\frac{1}{H\zeta}(\tfrac{1}{2} - \tfrac{2}{5}\zeta)^{\frac{1}{2}}. \tag{29}$$

Those solutions describing the properties of the thermals and environment are plotted in figure 9. In each case the form resembles the equivalent property of the plume.

An attempt was made to verify (28) in a simple experiment similar to those described for circular plumes. The same reservoir was used and thermals produced by droplets of salt water falling from the end of a 5 mm tube, 7 mm above the water surface. Most, but not all, of the droplets produced turbulent ring vortices upon impingement. After 7 h of operation the density distribution was measured and found to be in qualitative agreement with (28). The shape of the profile departed appreciably from the theoretical prediction, being less steep than indicated by (28) near $\zeta = 1$. The reason for this lack of agreement in detail was probably that too large a proportion of the thermals differed from the most common form, the ring vortex. Nevertheless, the agreement was sufficiently good to give confidence in the analysis.

5. Extensions of the method

We shall now show how the solutions obtained above can be modified to take into account other more realistic boundary conditions. The removal of the infinities introduced by the assumption of virtual point sources, the behaviour of pairs of sources, and the effect of an environment which has a changing cross-section with height will all be considered briefly here and illustrated by specific examples. The notation used will be the same as before.

5.1. *A well-mixed layer at the bottom of the environment*

Although the increasingly sharp gradients in the environment near the source are observed in the laboratory experiments, this is a feature which one would not expect to find in the atmosphere, for example. Instead, there will be a region near the ground which is well mixed or even unstably stratified, because of mechanical or convective mixing generated over the whole boundary. Let us suppose that a fraction δ of the heat flux goes into heating this lower layer, in the form of smaller elements whose behaviour we shall not consider in detail, while the remaining part continues upwards in the form of plumes to heat the upper part of the environment.

When a steady state is attained, it is clear from previous arguments that there will be a well-mixed layer of depth δH, on top of which is a layer $(1-\delta)H$ with

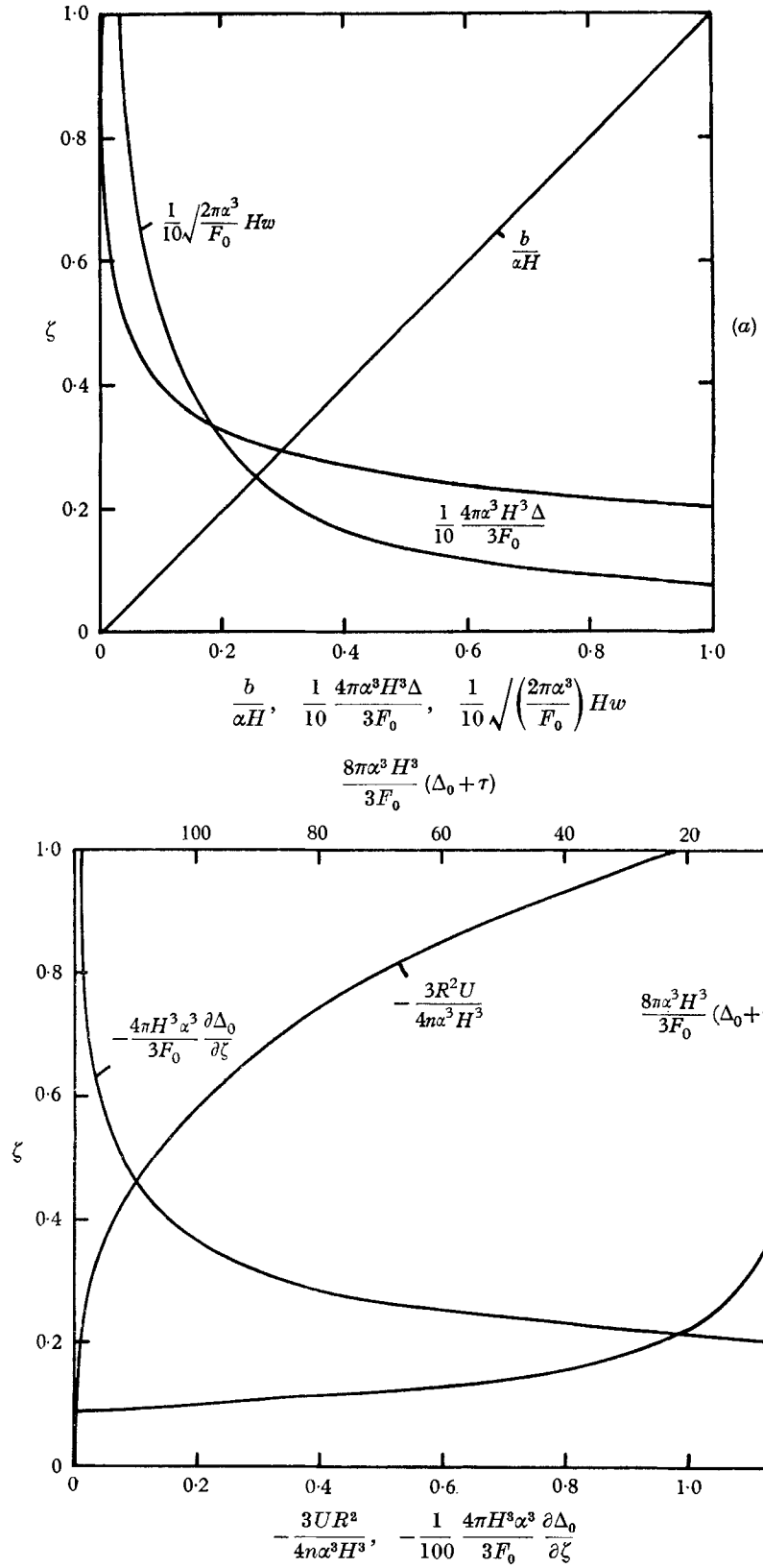

FIGURE 9. Asymptotic solutions for thermals in circular container. (*a*) Radius, velocity and density defect in plume. (*b*) Velocity, density defect and density gradient in environment.

a stable distribution of density formed by the plumes. The whole profile stays constant in shape while the temperature increases steadily in time. The density (but not the density gradient) must be continuous at δH. Although there will be a downward velocity and mixing into the bottom layer across this level, no net heat flux is associated with this process.

We shall take as our example the line plume, this being a structure commonly observed in the atmosphere under conditions of light wind (Priestley 1959). The corresponding modifications for other cases will be obvious. The reduction of the equations to non-dimensional form must be based as before on the total F_0 per unit length and H, in order to make comparisons with previous results, and the differences must lie in the boundary conditions and the way in which they are applied. It is again supposed that the whole environment is non-turbulent (a more questionable assumption now in the well-mixed layer), and that the plumes reaching the top of the environment arise from line buoyancy sources at the bottom boundary. At the height δH where our previous model becomes relevant, these will have the more realistic finite properties characteristic of a source of strength $(1-\delta)F_0$ per unit length, which has risen a distance δH in a *uniform* environment. The same equations (17) and (19) will therefore hold above this height but with boundary conditions

$$f = \delta^{-1}(1-\delta)^{\frac{2}{3}}, \quad j = \delta(1-\delta)^{\frac{1}{3}}, \quad x = \delta(1-\delta)^{\frac{2}{3}}, \quad \zeta = \delta. \tag{30}$$

A simple power series solution cannot be obtained in this case, because we are not starting near the power law solution in uniform surroundings. The equations are very simple to integrate numerically and when δ is small, the solutions, apart from the constant region in Δ_0 below $\zeta = \delta$, are virtually indistinguishable from those of figure 8. For example, if $\delta = 0{\cdot}1$ the only significant changes are a reduction in the plume velocity of 1 % and an increase in the density gradient of 1 % at the most as compared to the previous asymptotic solutions.

5.2. *Equal and opposite pair of sources*

The well-mixed layer near a source of buoyancy could be supplied by a source of opposite sign on the opposite surface. This is a situation easily realized in the laboratory and could occur in any of the large-scale examples whenever there is a source of negative buoyancy (which could also be called a buoyancy sink) on the top of the layer. If the two sources are of equal strength the environment in this case would approach a truly steady state, i.e. $\partial\Delta_0/\partial t = 0$. Inserting this value in the equation for conservation of Δ_0 produces a requirement that either the environment velocity U or density gradient $\partial\Delta_0/\partial z$ must be zero everywhere. This and the equation of continuity can be satisfied only if the environment becomes two layers of equal thickness as illustrated on figure 10. A similar picture was obtained by Gill (1966) for a laminar flow in a closed container with heated side walls. In this case, however, a continuous linear density gradient was developed in the interior due to the removal of fluid from the boundary layers over part of their length, an effect which does not occur for turbulent plumes.

The environment velocity is zero along $z = \frac{1}{2}H$ for reasons of symmetry, hence the fluid entrained into both plumes within a layer comes entirely from the plume

which ends in it. Self-entrainment by this plume produces the asymptotic state of uniform density, though during the earlier stages both layers will be stably stratified. A density difference must exist between the layers in order that the flux of buoyancy relation can be satisfied.

The plume equations also have simple solutions in this case. In the layer far from its source the plume must have the same density as its environment and hence be a constant momentum jet. Thus the fluid in the plume is accelerated in the first layer but not as it passes through the second.

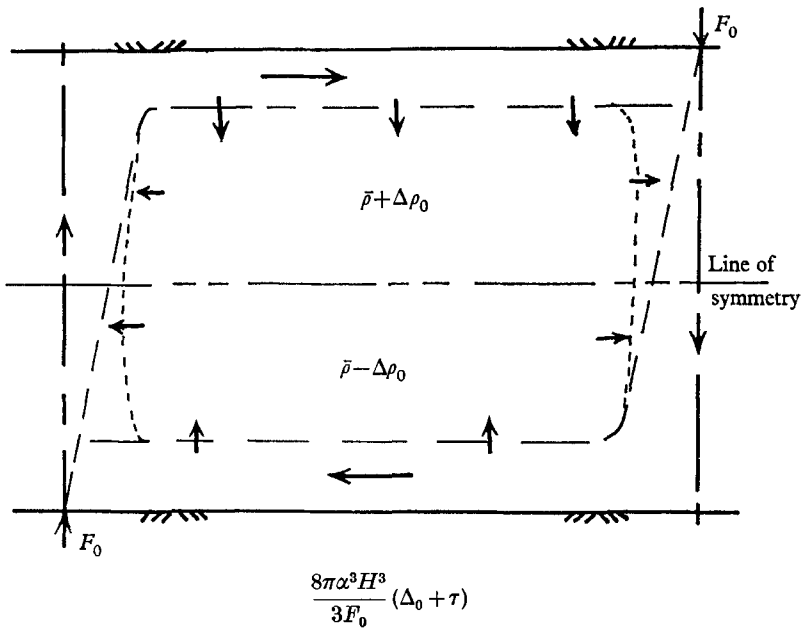

FIGURE 10. Sketch of environment produced by equal and opposite sources. Dashed line shows indicated limit for closely spaced plumes.

The density of the two layers can be obtained directly from the equations for a simple plume since $\Delta = 0$ in the far layer. In terms of the variables defined previously the density in the plume at the mid-plane is

$$\Delta_{0\cdot5} = \pm\sqrt{2}\left(\frac{F_0}{\alpha}\right)^{\frac{2}{3}}\frac{2}{H} \tag{31}$$

for line plumes and

$$\Delta_{0\cdot5} = \pm\frac{5}{3\alpha^{\frac{4}{3}}}\left(\frac{5}{18}\right)^{\frac{1}{3}}F_0^{\frac{2}{3}}\left(\frac{2}{H}\right)^{\frac{5}{3}}. \tag{32}$$

for circular plumes.

In each of these equations Δ is the difference in relative density between the plume and near layer. It is also the difference between the two layers because $\Delta = 0$ in the far layer, i.e.

$$\Delta_{0\cdot5} = 2g(\Delta\rho/\bar{\rho}). \tag{33}$$

If the plumes are close together these equations should not describe the density field since there would be a direct flow of fluid from one plume into the other near

the source. Such a flow would develop more readily than in the cases considered previously because the stabilizing influence of stratification is absent. For this to occur the ratio H/R would be expected to be larger than that resulting in instability for a single plume. By extending this general reasoning to cases of more closely spaced plumes a limiting case is obtained where all of the fluid from one enters the other without passing through the enrivonment, as shown in the dotted curve in figure 10. The plumes would thus be isolated from the environment which should remain at rest at a uniform density. As shown, however, by by Elder (1965) and Gill (1966) this state is not approached in practice; the flow in a narrow slot is considerably more complicated than that envisaged here, and its discussion lies outside the scope of the present model.

5.3. *Containers of different shapes*

For the large-scale examples mentioned in the opening sections of this paper, the assumption of a constant cross-section is a natural one. The container is envisioned as one cell of a very much larger horizontal layer. There are, however, applications of geophysical and laboratory interest in which the geometry is different. The hot, salty pool at the bottom of the Red Sea referred to in § 1 is contained in a shallow basin of irregular shape. This is presumed to be heated over a limited area at the bottom where the cross-section is small, but the basin widens continuously with height.

Let us consider a two-dimensional container of depth H with half width $R = R(z)$ heated by a line plume at $z = 0$. Any of the other cases can be treated by an identical development but for the sake of brevity they will not be considered here. The plume equations are not affected by the container shape nor is the conservation equation (4) for Δ_0. The only changes are in the interpretation of the equation of continuity in which now R is no longer a constant and in the definition of the rate of buoyancy addition

$$\frac{\partial \Delta_0}{\partial t} = -\frac{F_0}{2\int_0^H R\,dz}. \tag{34}$$

In the non-dimensional representation (16) is unchanged except that a representative lateral width must be specified in place of R. The most natural choice is R_1, the half width at the top. Equations (17a) to (17c) are unchanged by these revisions but (17d) becomes

$$j\frac{df_0}{d\zeta} = \frac{r}{\int_0^1 r\,d\zeta,} \tag{35}$$

in which r has been written for the dimensionless width $r = R/R_1$. Combining (35) with the buoyancy flux equation (17c), integrating and applying the boundary condition that at the top $\Delta = 0$ gives

$$fj = -\left\{1 - \left(\int_0^\zeta r\,d\zeta \Big/ \int_0^1 r\,d\zeta\right)\right\} = -(1 - V). \tag{36}$$

The pair of equations (19) is now replaced by the following in j and $x = -g^2h$

$$\left.\begin{aligned} j(dj/d\zeta) &= -x, \\ x(dx/d\zeta) &= -j(1-V); \end{aligned}\right\} \tag{37}$$

the only change is that the linear term in ζ has been replaced by a function which is the relative volume of the container below the level ζ.

Let us specialize still further, and calculate explicitly the properties produced in a wedge-shaped region with plane sloping sides by a line plume located along its vertex $\zeta = 0$. Here $r = \zeta$ so $V = z\int_0^\zeta r\,d\zeta = \zeta^2$. The same analysis holds for the family of wedges of different angles. This angle will affect the velocity and time scales through the ratio H/R_1 in the (modified) relations (16) but the other properties do not depend on it.

Series solutions can be obtained again in this case satisfying $f = 1$ and $x = j = 0$ at $\zeta = 0$; the first few terms are:

$$\left.\begin{aligned} x &= -\zeta(1-\tfrac{4}{15}\zeta^2+\tfrac{6}{25}\zeta^4), \\ j &= -\zeta(1-\tfrac{1}{15}\zeta^2+\tfrac{17}{450}\zeta^4), \\ f_0 &= 2\zeta(1+\tfrac{1}{45}\zeta^2-\tfrac{1}{450}\zeta^4)-2{\cdot}040. \end{aligned}\right\} \tag{38}$$

The solutions for all the non-dimensional functions calculated from these are shown in figure 11. The differences from the solutions of figure 8 in a rectangular box are striking. The density distribution is nearly linear with height, and the velocities in both the plume and the environment are almost constant (within 5 %). The plume fluid will, moreover, be recycled through the environment and return to the source in a *finite* time, which is in non-dimensional terms $\tau_1 = 2{\cdot}040$. (Compare this behaviour with the earlier relation (21)). The 'asymptotic' conditions should therefore also be achieved in actual physical cases. Furthermore, the experiments in the container with R constant indicated that the time to achieve this state is of the order of τ_1, whence the time to establish it for the wedge-shaped box should be of the order of τ_1, or less.

6. Practical applications

When one considers the physical cases in which this model could describe the heat or mass transfer it is apparent that most are horizontal layers of very large lateral extent compared to thickness. Rarely is the location or strength of buoyancy source specified; most often the flux per unit area of the lower surface F_A is the boundary condition. In terms of the quantities used for the point source this is

$$F_A = \frac{F_0}{\pi R^2} = -H\frac{\partial \Delta_0}{\partial t}$$

and a similar expression can also be obtained for line plumes and thermals.

The property of primary interest in many of these cases is the minimum density or temperature gradient which exists in the environment. For the container with uniform cross-section this occurred at the top and in dimensional variables is

$$\partial\Delta_0/\partial z|_{z=H} = 0{\cdot}66\alpha^{-\frac{4}{3}}F_A^{\frac{2}{3}}H^{-\frac{4}{3}}(R/H)^{\frac{1}{3}}. \tag{39}$$

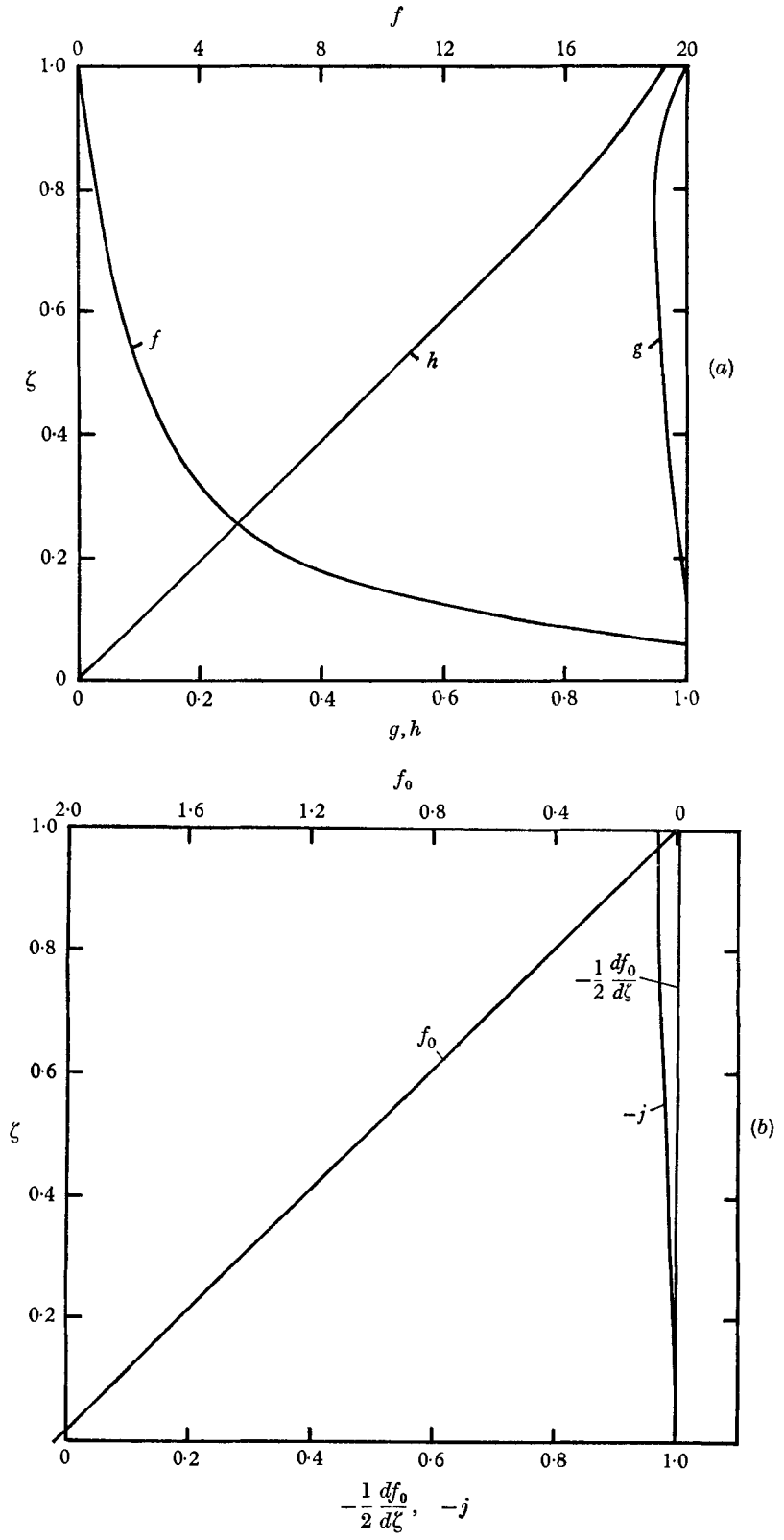

FIGURE 11. Asymptotic solutions for a line plume in a wedge-shaped container. (*a*) Plume variables defined by (16). (*b*) Environment variables defined by (16).

But consider further a typical atmospheric situation where temperature or temperature gradient is measured at a given height in the presence of a light wind. The quantity measured is not Δ or Δ_0 but an average of them. The measuring instrument integrates the temperature (or density defect) over the environment and the plumes as they pass by. In exact terms this average density is

$$\bar{\rho} = \left[\pi(R^2 - b^2)\rho_0 + \int_0^b \rho 2\pi r\, dr\right] \Big/ \pi R^2,$$

which in terms of the dimensional variables of § 3.3 is

$$\bar{f} = f_0 - 8\alpha^2 (H/R)^2 fh^2, \tag{40}$$

where the mean buoyancy defect

$$\bar{\Delta} = g\{(\bar{\rho} - \rho_1)/\rho_1\} = 2\pi^{\frac{2}{3}} F_0^{\frac{2}{3}} \alpha^{-\frac{4}{3}} H^{-\frac{5}{3}} (f(\zeta) - \tau).$$

The density gradient determined from averaged measurements at two closely spaced elevations is found by differentiating (40), giving

$$\frac{d\bar{f}}{d\zeta} = \frac{df_0}{d\zeta}\left[1 - 8\alpha^2 \left(\frac{H}{R}\right)^2 gh^2 \frac{d}{d\zeta}\left(\frac{1-\zeta}{g}\right)\right]. \tag{41}$$

The dimensionless term $-gh^2(d/d\zeta)((1-\zeta)/g)$ can be found from the solutions (13) and (14) discussed above; these expansions must however be carried to five terms to allow it to be determined accurately. We find that the term is zero at $\zeta = 0$, reaches a small negative maximum, and is zero again about $\zeta = 0{\cdot}3$. Above this value it is positive, reaching 0·4 at $\zeta = 1$. This means that the full correction term is no larger than 0·04 assuming that $\alpha = 0{\cdot}1$ and $H/R \leqslant 1$. The mean gradient is therefore always stable and within 4 % of that in the environment.

For line sources the corresponding results are calculated in the same way. The minimum density gradient is

$$\left.\frac{\partial \Delta_0}{\partial z}\right|_{z=H} = 1{\cdot}462\alpha^{-\frac{2}{3}} F_A^{\frac{2}{3}} H^{-\frac{4}{3}} \left(\frac{R}{H}\right)^{\frac{2}{3}}. \tag{42}$$

The average density at elevation ζ is given by

$$\bar{f} = f_0 - \frac{\alpha}{\sqrt{2}} \frac{H}{R} fh, \tag{43}$$

where the mean buoyancy defect

$$\bar{\Delta} = 2^{-\frac{1}{2}} F_0^{\frac{2}{3}} \alpha^{-\frac{2}{3}} H^{-1} (\bar{f}(\zeta) - \tau).$$

From (20) it is easily seen that $fh \approx 1 - \zeta$ and from considerations of stability $(H/R) \leqslant 1$ so the whole correction term must be negative and small (note that a value of $\alpha = 0{\cdot}065$ for line plumes with Gaussian profiles can be taken from Ellison & Turner (1959)). The average density is therefore slightly less than that in the environment. The average density gradient has the opposite trend. Differentiation of (38) gives

$$\frac{d\bar{f}}{d\zeta} = \frac{df_0}{d\zeta}\left(1 - \frac{\alpha}{\sqrt{2}} \frac{H}{R} gh \frac{d}{d\zeta}(fh)\right). \tag{44}$$

The dimensionless function $-ghd(fh)/d\zeta$ is readily shown to be positive for $0 \leqslant \zeta \leqslant 1$ and thus the correction term augments the stable gradient in the environment. However, it is not possible to determine the term with accuracy because of the limited number of terms in our series solution. It is roughly proportional to ζ and the maximum value is less than 0·9. The maximum value for the whole term is thus of the order of 0·04. Such a correction is unlikely to affect results in most practical situations and the environment gradient can therefore be taken to be the average gradient.

As demonstrations of this model let us consider some of the examples mentioned in § 1. Numerical values are inserted directly in (39) or (42).

6.1. *Cooling of a room by a line source*

Suppose that a room 3 m high and 6 m wide is being cooled at the rate of 20° C/h by a single cold line source running along the centre of the ceiling. Neglecting losses the physical quantities are (in c.g.s. units), $\partial\Delta_0/\partial t = 2 \times 10^{-2}$, $H = 3 \times 10^2$, $R/H = 1$ so $\partial\Delta_0/\partial z \approx 10^{-2}$ which corresponds to a temperature gradient of 0·4 °C/m near the floor. About 30 cm from the ceiling the gradient would be ten times as great.

6.2. *Heating of the atmosphere below cloud-base*

If $H = 1$ km and this layer of air is heated by equal point sources spaced to give $R \approx H$ then with a heating rate of 1 °C/h,

$$\partial\Delta_0/\partial t = 10^{-3}, \quad H = 10^5, \quad \partial\Delta_0/\partial z|_{\text{max.}} = 6{\cdot}5 \times 10^{-5},$$

which implies a stable potential temperature gradient of 2 °C/km. Warner & Telford (1967) suggested a mean value of about $\frac{1}{10}$ of this in the lower atmosphere under convective conditions—but of course we have not taken into account the effect of closer plume spacing which was indicated by the measurements, or of a distribution of plume strengths which would also have the effect of decreasing the gradients.

6.3. *Cooling of the 'upper mixed layer' in the ocean*

Convection in the surface layer of the ocean above the seasonal thermocline has usually been considered to take place in the form of a series of overturning cells. If the process is interpreted instead as a series of rectangular sections being filled by line plumes spaced 50 m apart our model gives the following results for a cooling rate of 0·05 °C/h: $\partial\Delta_0/\partial t = 2 \times 10^{-6}$, $H = 2 \times 10^3$, $R/H = 1{\cdot}25$ so $\partial\Delta_0/\partial z|_{\text{max.}} = 1 \times 10^{-5}$ which corresponds to a minimum temperature gradient of 7×10^{-5} °C/cm and a difference of about 0·3 °C between the bottom of the layer and a depth of 2 m.

6.4. *Heating of a wedge-shaped basin*

As an idealized version of the basin at the bottom of the Red Sea, consider a wedge-shaped contained with a depth of 100 m and a top width of 4 km whence $R_1/H = 20$. If this is heated by a line source at the bed (16) and (38) give

$$\frac{\partial\Delta_0}{\partial z} = 1{\cdot}59\alpha^{-\frac{2}{3}}\left(\frac{\partial\Delta_0}{\partial t}\right)^{\frac{2}{3}}\left(\frac{R_1}{H}\right)^{\frac{2}{3}}H^{-\frac{2}{3}}. \tag{45}$$

Suppose the whole basin is heating at a rate of 0·3 °C/year so that

$$\partial\Delta_0/\partial t = 4\times10^{-9}$$

(using a coefficient of expansion appropriate to 50 °C). Then $\partial\Delta_0/\partial z = 4\times10^{-7}$, corresponding to a potential temperature gradient of 10^{-6} °C/cm, i.e. 0·1 °C/km. Stable gradients about ten times as large as this have in fact been observed, with the assumed overall heating rate. This suggests an explanation in terms of more concentrated sources, not a line source down the whole of the basin; the assumption of either a short line source, or a point source, will have the effect of increasing the importance of the (R_1/H) term. A more detailed calculation, using the observed bathymetry of the basin, might in fact allow one to make some predictions about the extent of the sources which could produce the observed gradient and rate of heating.

7. Final remarks

In conclusion, we should review the main features of the model developed herein, but with a warning about effects which have been so far ignored in its development, and which may limit its range of direct application. Concurrently the possible extensions will also be mentioned. The excellent agreement between the theoretical model and the laboratory experiment leave no doubt that the process of 'filling a box with a plume' (or other convective elements) can lead to the production of a stable gradient, whose form is calculable when the distribution of sources is known. This gradient is stable, moreover, when horizontal averages are taken including the plumes as well as the 'environment', and the model gives a clear physical explanation for the phenomenon of 'transport against the gradient'. It can be modified satisfactorily to remove the unreal infinities associated with point sources, and to take account of a well-mixed layer near the source.

The model has left out entirely the effect of turbulence in the environment. Some of its basic features (such as the reversed gradient) are still present however in laboratory experiments on turbulent convection, and even in the real atmosphere. It is therefore suspected that turbulence produces a quantitative rather than a qualitative change in the results, although the problem of describing the mixing in both directions between a turbulent element and its turbulent surroundings has not yet been solved properly. Another assumption which may be unrealistic for the real atmosphere is the use of fixed rigid walls bounding the part of the environment in which convection is occurring. Often the boundary at its top is rising as the increasing temperature of the surface layer overtakes that in the inversion above; this too could be, but has not yet been, incorporated into a 'filling box' model. The transport of heat by conduction from this top surface could also be included.

It is tempting to try to interpret many meteorological and oceanographic phenomena, covering a very wide range of scales, in terms of a model of this kind. Thus the general subsidence of the atmosphere and the upwelling in the ocean can be thought of respectively as the result of more limited regions of upflow

(in cumulonimbus clouds) and downflow (in Arctic regions). The atmospheric case is complicated by losses due to radiation, but for the ocean it is known that all the heat is put in and removed near the surface, and that the 'bottom water' is formed in a few very small areas. A time-dependent filling box model, which preserves the mean temperature profile while mixing is accomplished by plumes which penetrate to varying depths seems worth exploring theoretically. Its feasibility was demonstrated in a laboratory experiment with an oscillating source. The simpler case of two steady sources of different strengths has also been studied in a laboratory experiment. It was observed that the weaker plume terminated at an elevation within the environment and that the density profile was similar to that produced by a single plume. No analytic model has yet been devised which produces solutions for comparison to the measurements in either of these cases.

Finally, we mention the most important limitation of all, the need to specify the type, strength and separation of the sources for the application of our results. In most situations of interest convection begins from a more uniform distribution of heating than the isolated sources considered, and the buoyant elements often arise spontaneously rather than associated with special features of the lower surface. In this case (and also in the case of more regularly spaced extended sources) lateral inflows must develop along the boundary. These are analogous to the well-mixed layers of § 5·1 in that they provide a mechanism for the elimination of the singularity at $\zeta = 0$ in the theoretical solution. The detailed understanding of the process of initial formation of the convection elements remains a major problem.

The first author held a Senior Research Fellowship from the National Research Council of Canada, during the period of this work, and the second was supported by a grant from the British Admiralty.

REFERENCES

ELDER, J. W. 1965 Laminar free convection in a vertical slot *J. Fluid. Mech.* **23**, 77–98.

ELLISON, T. H. & TURNER, J. S. 1959 Turbulent entrainment in stratified flows. *J. Fluid Mech.* **6**, 423–48.

GILL, A. E. 1966 The boundary-layer régime for convection in a rectangular cavity. *J. Fluid Mech.* **26**, 515–36.

GILLE, J. 1967 Interferometric measurement of temperature gradient reversal in a layer of convecting air. *J. Fluid Mech.* **30**, 371–84.

HERRING, J. R. 1964 Investigation of problems in thermal convection. *J. Atmos. Sci.* **21**, 277–90.

MORTON, B. R. 1959 Forced plumes. *J. Fluid Mech.* **5**, 151–63.

MORTON, B. R., TAYLOR, G. I. & TURNER, J. S. 1956 Turbulent gravitational convection from maintained and instantaneous sources. *Proc. Roy. Soc.* A **234**, 1–23.

PRIESTLEY, C. H. B. 1959 *Turbulent Transfer in the Lower Atmosphere.* University of Chicago Press.

PUGH, D. T. 1969 Temperature measurements in the bottom layers of the Red Sea basins. Chapter in: *Hot brines and Recent Heavy Metal Deposits in the Red Sea.* Ed. E. T. Degers, D. A. Ross. New York: Springer-Verlag.

ROUSE, H., YIH, C. S. & HUMPHREYS, H. W. 1952 Gravitational convection from a boundary source. *Tellus* **4**, 201–10.

SCHWIND, R. G. & VLIET, G. C. 1964 Observations and interpretations of natural convection and stratification in vessels. *Proc. Heat Transf. and Fluid Mech. Inst.* 51–68.

TURNER, J. S. 1963 The motion of buoyant elements in turbulent surroundings. *J. Fluid Mech.* **16**, 1–16.

WARNER, J. & TELFORD, J. W. 1967 Convection below cloud base. *J. Atmos. Sci*, **24**, 374–82.

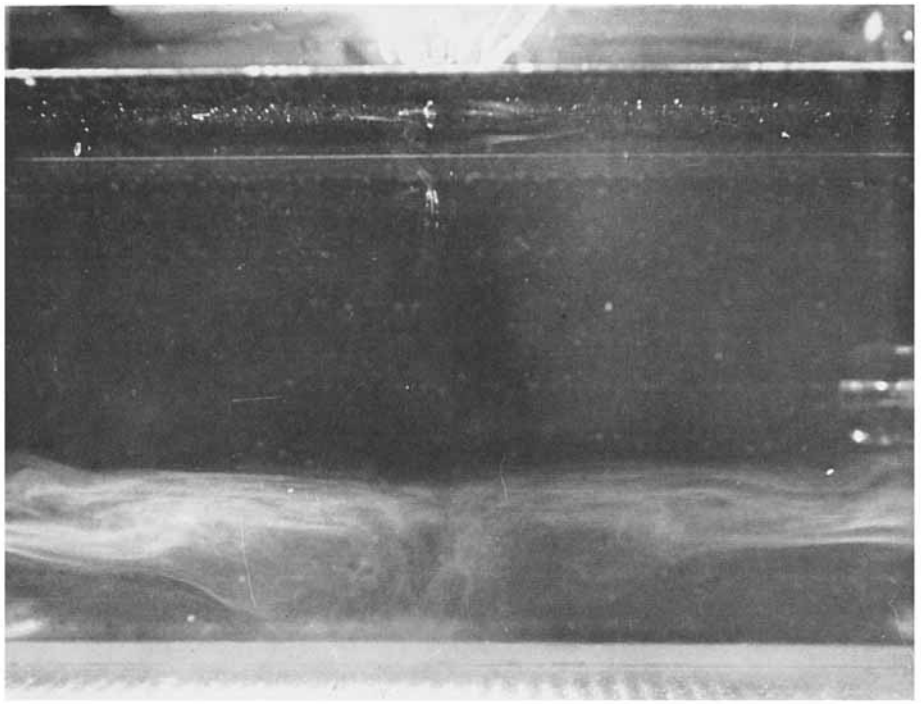

(*a*)

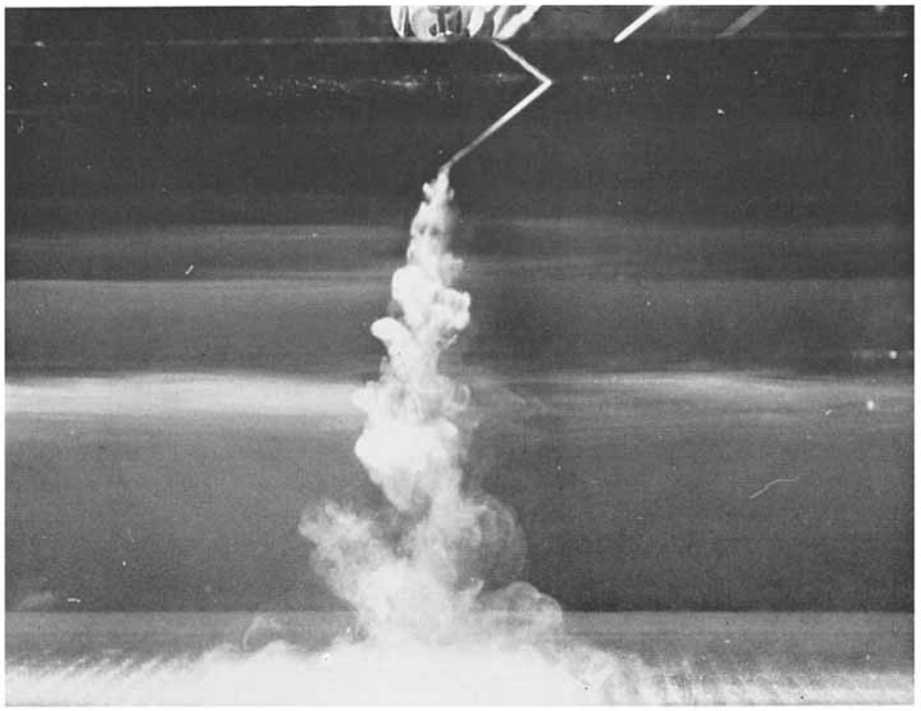

(*b*)

FIGURE 1. (*a*) Establishment of the first front by a circular plume. (*b*) Later development of stratified environment. Dyed layers were produced by injections at constant time intervals in the past.